Spectral Factorization in Periodically Time-Varying Systems and Application to Navigation Problems

T. NISHIMURA*
Jet Propulsion Laboratory, Pasadena, Calif.

Spectral factorization is a powerful tool in deriving the steady-state solution of Kalman filtering equations. It is an algebraic, nonrecursive method, thus economical in terms of computing cost, when compared with the conventional iterative algorithm. In this paper the technique is extended to time-varying systems having periodic coefficient matrices for both discrete and continuous systems. The tracking of low-thrust spacecraft from an Earth-based station is used as an example and a sensitivity study is performed using a computer program incorporating the algorithm.

Introduction

KALMAN filters[1] have been widely employed for tracking of spacecraft in various interplanetary missions. Two-way or three-way Doppler links between spacecraft and Earth-based tracking stations have been the major source of information in determining spacecraft coordinates. Ranging has also played an important role in recent years.

Unmodeled random accelerations acting on the spacecraft introduce inaccuracies in these orbit determination problems. Examples of such accelerations are random fluctuations of solar pressure and leakage from attitude control valves during ballistic missions and small perturbations in thrust level in the case of low-thrust missions. Because of such unmodeled accelerations, orbit determination precision reaches a minimum, some time after the start of tracking; then improvement in precision cannot be expected unless the spacecraft Earth station geometry changes significantly or a new type of information, such as range data, is supplied.

Therefore it is of utmost importance to find out such limiting accuracies for the particular tracking system. One way of determining these limiting values is to run the sequential filtering program long enough on the computer until the covariances reach a steady state. However, this may be very expensive if the convergence of filters is very slow.

Analytic solutions[2,3,4] employ eigenvector, eigenvalue subroutines in finding the steady-state solution of Kalman filters without iteration for constant coefficient systems. This approach is called spectral factorization because it corresponds to the same operation in static filters. In this paper, the spectral factorization algorithm is extended to periodically time-varying cases for both discrete and continuous systems.

Spectral Factorization for Periodically Time-Varying Systems

The dynamic equation for the parameter vector $x(n \times 1)$ and the equation for the observable $y(m \times 1)$, for discrete systems are:

$$x(k+1) = \Phi(k)x(k) + G(k)w(k) \tag{1}$$

$$y(k) = H(k)x(k) + n(k) \tag{2}$$

where w and n are independent, white noises with zero mean. Hence

$$E[w(k)w(j)'] = Q(k)\delta_{kj} \tag{3}$$

$$E[v(k)v(j)'] = R(k)\delta_{kj} \tag{4}$$

and δ_{kj} is the Kronecker delta and $E[\ ]$ indicates an ensemble average.

The error covariance $P(k)$ of the optimal estimate of $x(k)$ is provided by[1]:

$$P(k+1) = \Phi(k)\{P(k) - P(k)H'(k)[H(k)P(k)H'(k) + R(k)]^{-1} \cdot H(k)P(k)\}\Phi'(k) + G(k)Q(k)G(k)' \tag{5}$$

with the initial condition:

$$P(0) = E[x(0)x'(0)] \tag{6}$$

Equation (5) converges to a unique steady-state solution, provided the system is uniformly observable and controllable.[1] Assuming this observability and controllability condition is satisfied, this unique steady-state solution is derived in Ref. (3) for the case when the system is time-invariant and noises are stationary by means of the canonical decomposition of the Riccati equation. Specifically, Eq. (5) reduces in this case to

$$P = \Phi\{P - PH'(HPH' + R)^{-1}HP\}\Phi' + GQG' \tag{7}$$

Let a matrix $A(2n \times 2n)$ be constructed by the coefficient matrices of Eq. (7) such that

$$A = \left[\begin{array}{c:c} \Phi + GQG'\Phi'^{-1}H'R^{-1}H & GQG'\Phi'^{-1} \\ \hdashline \Phi'^{-1}H'R^{-1}H & \Phi'^{-1} \end{array}\right] = \left[\begin{array}{c:c} A_{11} & A_{12} \\ \hdashline A_{21} & A_{22} \end{array}\right] \tag{8}$$

Also let $T(2n \times 2n)$ be a matrix of eigenvectors of A and let it be partitioned similar to A. Then the solution of Eq. (7) is obtained in Ref. (3), as described by the following theorem.

Theorem 1 Steady-State Solution for Discrete Time-Invariant Systems

A real, symmetric, non-negative definite solution of P of Eq. (7) can be uniquely determined by arranging the submatrix $[T_{11} \vdots T_{21}]$ such that it consists of eigenvectors of A, corresponding to eigenvalues that lie outside the unit circle around the origin of the complex plane, assuming all the eigenvalues of A are distinct and not lying on the unit circle. Then P is computed as a ratio of T_{11} and T_{21}, assuming that T_{21} is nonsingular:

$$P = T_{11}T_{21}^{-1} \tag{9}$$

Received September 5, 1971; revision received March 6, 1972. This paper represents one phase of research carried out at the Jet Propulsion Laboratory, California Institute of Technology, under NASA Contract NAS 7-100.

Index categories: Spacecraft Navigation, Guidance, and Flight Path Control Systems; Spacecraft Tracking; Navigation, Control and Guidance Theory.

* Member of Technical Staff.

In this paper the algorithm is extended to time-varying systems having periodic coefficient matrices for both discrete and continuous systems. Let the matrices $\Phi(k)$, $H(k)$, $G(k)$, $R(k)$, and $Q(k)$ in Eq. (5) be periodically varying in time, with period L. Then, the steady-state solution of Eq. (5) is also expected to be periodic, with the same period L. Such a periodic solution is provided by the following theorem. Let the matrix $B(k, 0)(2n \times 2n)$ be constructed by

$$\begin{aligned} &B(k, 0) = A(k-1)A(k-2)\dots A(0),\ 0 \leq k \leq L \\ &B(0, 0) = \mathrm{I} \qquad\qquad (\mathrm{I}: \text{an identity matrix}) \end{aligned} \tag{10}$$

where $A(i)$ is given by Eq. (8) in which all the matrices are taken at the ith instant. Also let $T(L)(2n \times 2n)$ be a matrix whose columns are composed of eigenvectors of

$$B(L, 0) = A(L-1)A(L-2)\dots A(0) \tag{11}$$

and let its left half $[T_{11}(L)\,|\,T_{21}(L)]$ be composed of eigenvectors corresponding to eigenvalues outside the unit circle around the origin, on the complex plane, assuming all eigenvalues are distinct and not lying on the unit circle.

Theorem 2 Steady-State Solution for Discrete Periodic Systems

A periodic steady-state solution of Eq. (5) at the instant L, assuming that $T_{21}(L)$ is nonsingular, is given by:

$$P(L) = T_{11}(L)T_{21}(L)^{-1} \tag{12}$$

At other instants

$$\begin{aligned} P(L+k) = &[B_{11}(k, 0)T_{11}(L) + B_{12}(k, 0)T_{21}(L)] \\ &\cdot [B_{21}(k, 0)T_{11}(L) + B_{22}(k, 0)T_{21}(L)]^{-1} \\ &k = 0, 1, 2, \dots, L-1 \end{aligned} \tag{13}$$

The proof of Theorem 2 is given in the Appendix. The solution matrix $P(L+k)$ given by Eqs. (12) and (13) is a real, symmetric and non-negative definite matrix and it is a unique solution of Eq. (5) with periodic coefficients. These properties of $P(L+k)$ can be proved in a manner similar to the proof of Theorem 1 given in Ref. 3. Furthermore, the results of Theorem 2 can be extended with minor modifications, to continuous systems.

Extension to Continuous Systems

The process equation and the observation equation for continuous systems are, respectively:

$$dx(t)/dt = F(t)x(t) + G(t)w(t) \tag{14}$$

$$y(t) = H(t)x(t) + n(t) \tag{15}$$

The covariance $P(t)$ of estimate $x^*(t)$ is given by the following equation

$$\begin{aligned} dP/dt = &F(t)P(t) + P(t)F'(t) - \\ &P(t)H(t)'R(t)^{-1}H(t)P(t) + G(t)Q(t)G'(t) \end{aligned} \tag{16}$$

When the coefficient matrices F, G, H, Q, and R are periodic, with period t_p, the steady-state periodic solution of Eq. (16) can be obtained analogous to the discrete case.†

Only the final results are given in this section. Let the transition matrix $B(t, s)(2n \times 2n)$ be defined by

$$\begin{aligned} &dB(t,s)/dt = A(t)B(t,s) \\ &B(s,s) = I \qquad\qquad t \geq s \geq 0 \end{aligned} \tag{17}$$

where A matrix $(2n \times 2n)$ is constructed as

$$A(t) = \begin{bmatrix} F(t), & GQG'(t) \\ H'R^{-1}H(t), & -F'(t) \end{bmatrix} \tag{18}$$

† When these coefficient matrixes were constant, the steady-state solution was derived by Potter.[4]

Let $T(t_p)$ be a $(2n \times 2n)$ matrix composed of eigenvectors of $B(t_p,0)$ and let its left half $T_{11}\,|\,T_{21}$ be composed of eigenvectors corresponding to eigenvalues having positive real parts, assuming that all the eigenvalues are distinct and not lying on the imaginary axis on the complex plane.

Theorem 3 Steady-State Solution for Continuous Periodic Systems

A periodic steady-state solution of Eq. (16) is given by

$$P(t_p) = T_{11}(t_p)T_{21}{}^{-1}(t_p) \tag{19}$$

and

$$\begin{aligned} P(t+t_p) = &[B_{11}(t,0)T_{11}(t_p) + B_{12}(t,0)T_{21}(t_p)] \\ &[B_{21}(t,0)T_{11}(t_p) + B_{22}(t,0)T_{21}(t_p)]^{-1} \end{aligned} \tag{20}$$

This theorem can be proved by steps similar to the case of discrete systems; however, the proof is not presented in this paper.

Information Content of Doppler Data

It is well-known that the "velocity parallax" effect, due to the tracking station's rotation with the Earth, enables us to determine the position of a distant spacecraft, in the directions of right ascension and declination, by means of two-way Doppler tracking. The major information content of Doppler data may be expressed as[5]

$$\dot{\rho} = a + b \sin \omega t + c \cos \omega t \tag{21}$$

where (see Fig. 1) $\dot{\rho}$ = Doppler data; a = geocentric radial velocity; $b = (-\omega r_s \cos \delta)$; $c = (\omega r_s \alpha \cos \delta)$; ω = rotation rate of the Earth; r_s = distance between the station and the spin axis of the Earth; and α = right ascension of the spacecraft; δ = declination of the spacecraft.

Equation (21) indicates that the range rate of a spacecraft, which is moving with a constant speed radially away from the Earth, is composed of one constant parameter (radial velocity) and two periodically time varying parameters (Fig. 2). Fixing a Cartesian coordinate system, as shown in Fig. 1, at the starting time of tracking, the instantaneous position and velocity of a low-thrust spacecraft is described by:

$$\bar{x}((k+1)T) = \Phi\bar{x}(kT) + G\bar{w}(kT) \tag{22}$$

where

$$\bar{x} = (x, y, z, \dot{x}, \dot{y}, \dot{z})' \tag{23}$$

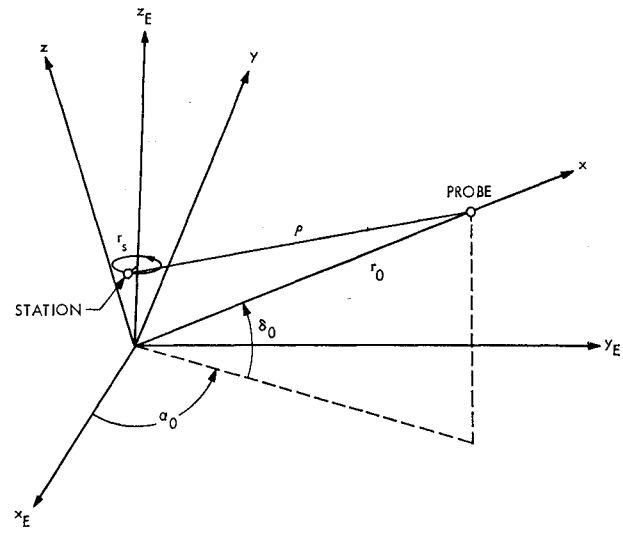

Fig. 1 Geocentric coordinate system.

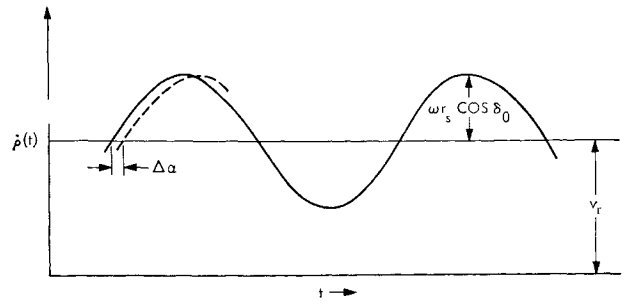

Fig. 2 Typical Doppler data pattern.

$$\Phi = \begin{bmatrix} I & T \cdot I \\ 0 & I \end{bmatrix}; \quad I = (3 \times 3) \text{ identity matrix} \tag{24}$$

$\bar{w} = (w_x, w_y, w_z)'$(3 components of random acceleration)
$T =$ discrete period.

On the other hand, the information y, which is a deviation of the range-rate from its nominal value, is given by

$$y(kT) = H(kT)\bar{x}(kT) + n(kT) \tag{25}$$

where

$$H(kT) = [0, \beta \sin \omega(kT), \gamma \cos \omega(kT), 1, 0, 0]; \tag{26}$$

$n(kT)$: data noise

$\beta = (\omega r_s/r_0) \cos \delta_0$; $\gamma = (-\omega r_s/r_0) \sin \delta_0$
$r_0 =$ geocentric range of spacecraft at t_0
$\delta_0 =$ declination of spacecraft at t_0

We observe in Eqs. (24) and (26) that the transition matrix Φ is constant, but the observation matrix is periodic (with the period equal to the single pass-width of data). Therefore, the result of Theorem 2 can be applied to the system described by Eqs. (22) and (25), in order to obtain the steady solution of the Riccati equation.

The range of magnitude of the process noise discussed in this paper is $10^{-8} \sim 5 \times 10^{-3}$ cm/sec^2 where[6]

$\sigma_w = 10^{-7} \sim 10^{-6}$ cm/sec^2	ballistic range, where the acceleration due to random solar disturbance and gas leakage are of this order.
$\sigma_w = 0.5 \times 10^{-4} \sim 0.5 \times 10^{-3}$ cm/sec^2	low-thrust range, where errors of thrust power of the solar electric engine are of this order.

Computer Program and Numerical Results

A computer program was developed in which Theorem 2 was applied to the periodically time-varying system described by Eqs. (22) and (25). First, the matrix A in Eq. (8) was obtained, using the Φ, H, Q, and R matrices defined in Eqs. (1–4). Then, the product of the A matrices over one pass of tracking (a 12 hr pass was used in this paper) was computed as the B matrix in Theorem 2.

Existing complex eigenvalue, eigenvector subroutines were applied to this B matrix and the associated eigenvalues and eigenvectors were obtained. Then one half of the eigenvectors corresponding to the eigenvalues lying outside the unit circle were used to form a submatrix $[T_{11}|T_{21}]$. Finally the matrix ratio $T_{11}T_{21}^{-1}$ was computed as the steady-state solution $P(L)$ of the tracking system described by Eqs. (22) and (25).

Further, an ordinary sequential program was built in which Eq. (5) was solved iteratively, starting from certain a priori covariance matrix, in order to verify the results of the spectral factorization program. Table 1 shows an example of comparison between these two programs.

Table 1 indicates a 3-place agreement of numbers and more precise agreement can be expected if computation of the sequential program is continued beyond 400 passes. However, even for 400 passes, the computing cost of the sequential program was 20 times larger than that of the spectral factorization program. This proves the accuracy as well as efficiency of the latter.

It is worthwhile to mention that a $5 \sim 10\%$ agreement was reached after 200 passes. Hence the computation cost for the sequential program would be at least 10 times as much as that of the spectral factorization program. The steady-state solution during the period can be computed by Eq. (13) after having obtained the values at L by Eq. (12). Since the major portion of computing time of this program is consumed in finding eigenvalues and eigenvectors, the additional computing cost required by matrix division in Eq. (13) is relatively small since eigenvectors have already been derived in Eq. (12).

In general, the settling time of the sequential program is closely related to the eigenvalues of the B matrix, since they dominate the transient performance of the filter.[4] If an eigenvalue of B is described by

$$\lambda_i = \alpha_i + j\beta_i \qquad i = 1, \ldots 2n \tag{27}$$

then the transient of the filter becomes a function of $(\lambda_i)^k$, $i = 1, \ldots 2n$, at time kLT. Therefore the settling time t_s of the filter may be defined as

$$t_s = \max_i [2/\log (\alpha_i^2 + \beta_i^2)] \cdot LT \tag{28}$$

This t_s was used as the maximum running time of the sequential program.

Using this spectral factorization program, various sensitivity studies are made, varying parameters such as standard deviations of process noise and data noise, correlation time of process noise and the radial distance to the probe and the results are depicted in Figs. 3–8.

Analysis of Rectilinear Motion and Sensitivity Study

Although the Doppler data taken at the ground station essentially supplies the information on the radial velocity of the probe, it also contains some information on the lateral position in the direction of right ascension, as well as of declination [b and c in Eq. (21)]. Such positional information plays the role of range data in the lateral directions.

Table 1 Comparison between spectral factorization and sequential program[a]

	σ_y(km)	σ_z(km)	$\sigma_{\dot{x}}$(mm/sec)	$\sigma_{\dot{y}}$(mm/sec)	$\sigma_{\dot{z}}$(mm/sec)
Spectral factorization	508.755	575.172	0.803337	8.65450	9.01646
Sequential program	508.952	575.397	0.803331	8.66149	9.02821

[a] Throughout this paper we assume that the radial distance x to the spacecraft is known accurately at the beginning of tracking by means of ranging; hence, a small a priori value is assigned to σ_x when the sequential program is used.

Therefore, a simplified analysis of a ranging system for a probe in rectilinear motion is useful in acquiring an insight into the basic structure of the tracking system discussed in this paper and a sensitivity study may be performed analytically using such a model.

Let the position and speed of a spacecraft in rectilinear motion be η and $\dot{\eta}$, respectively, and let us assume that the range data y is supplied at every interval T. Then the process and data equations for such a tracking system are:

$$\eta[(k+1)T] = \eta(kT) + T\dot{\eta}(kT) \tag{29}$$

$$\dot{\eta}[(k+1)T] = \dot{\eta}(kT) + w(kT)T \tag{30}$$

$$y(kT) = h\eta(kT) + n(kT) \tag{31}$$

where η and $\dot{\eta}$ are, respectively, the position and speed of the spacecraft and w and n are process noise and data noise, with respective standard deviations σ_w and σ_n. The data partial h is assumed constant. Then, a discrete Kalman filter for this system may be designed according to Ref. (1), and the error covariance P is provided by Eq. (5), and its steady-state equation by Eq. (7).

Let η^* and $\dot{\eta}^*$ be the estimates of η and $\dot{\eta}$, respectively, and let

$$p_{11} = E[(\eta^* - \eta)^2] \tag{32}$$

$$p_{12} = E[(\eta^* - \eta)(\dot{\eta}^* - \dot{\eta})] \tag{33}$$

$$p_{22} = E[(\dot{\eta}^* - \dot{\eta})^2] \tag{34}$$

Then from Eq. (7)

$$p_{11} = [h^2T^2(p_{11}p_{22} - p_{12}^2) + \sigma_n^2(p_{11} + 2Tp_{12} + T^2p_{22})]/\Delta \tag{35}$$

$$p_{12} = [h^2T(p_{11}p_{22} - p_{12}^2) + \sigma_n^2(p_{12} + p_{22}T)]/\Delta \tag{36}$$

$$p_{22} = [h^2(p_{11}p_{22} - p_{12}^2) + \sigma_n^2p_{22}]/\Delta + \sigma_w^2T^2 \tag{37}$$

where

$$\Delta = h^2p_{11} + \sigma_n^2 \tag{38}$$

Further manipulations of Eqs. (32–38) yield

$$p_{11}^4 = \sigma_w^2T^4(p_{11} + \sigma_n^2/h^2)(p_{11} + 2\sigma_n^2/h^2)^2 \tag{39}$$

$$p_{12} = \sigma_wT(p_{11} + \sigma_n^2/h^2)^{\frac{1}{2}} \tag{40}$$

$$p_{22} = \sigma_w(p_{11} + p_{12}T)/(p_{11} + \sigma_n^2/h^2)^{\frac{1}{2}} \tag{41}$$

Under certain assumptions several important conclusions can be drawn from these equations:

I Case of $p_{11} \ll \sigma_n^2/h^2$

Under this assumption

$$\hat{\sigma}_\eta[= (p_{11})^{\frac{1}{2}} \sim \sigma_w^{\frac{1}{2}}\sigma_n^{3/4}T^{\frac{1}{2}}/h^{3/4} \tag{42}$$

$$\hat{\sigma}_{\dot{\eta}} = (p_{22})^{\frac{1}{2}} \sim \sigma_w^{3/4}\sigma_n^{\frac{1}{2}}T^{3/4}/h^{3/4} \tag{43}$$

In other words: 1) Standard deviation of positional estimate is proportional to; a) fourth root of standard deviation of process noise, and b) three-fourth power of standard deviation of data noise; and 2) standard deviation of speed estimate is proportional to: a) three-fourth power of standard deviation of process noise, and b) fourth root of standard deviation of data noise.

The most important result is 1a and this can be seen in Fig. 3 because, in the ballistic range of σ_w, the inclination of curves is approximately 1/4. This confirms that $\hat{\sigma}_{y,z} \sim \sigma_w^{\frac{1}{4}}$. Also Fig. 4 shows that $\hat{\sigma}_{\dot{y},\dot{z}} \sim \sigma_w^{3/4}$ in the same range of σ_w.

Although these figures are the results of spectral factorization applied to the general three-dimensional problem, the analysis of the rectilinear one-dimensional case can be used qualitatively for the purpose of sensitivity study.

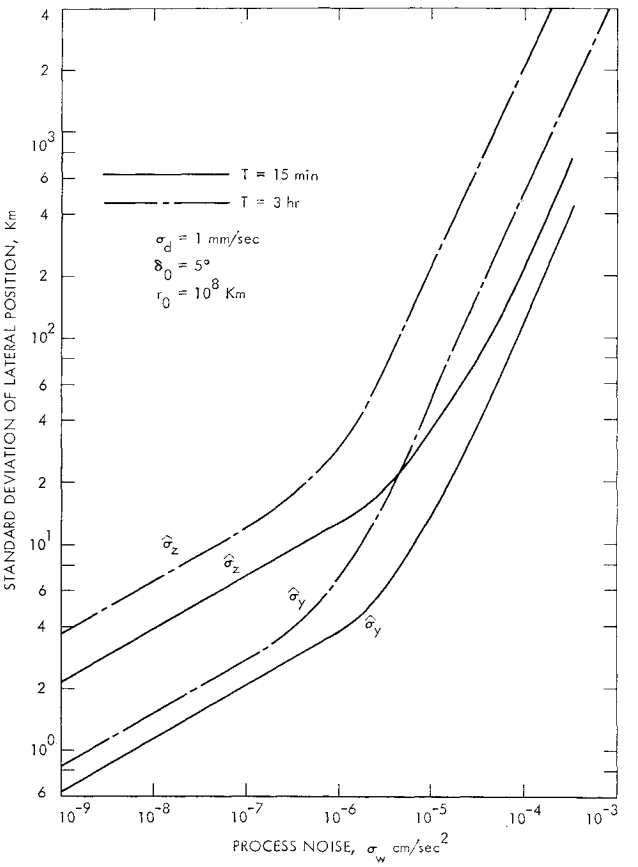

Fig. 3 Lateral position uncertainty vs process noise.

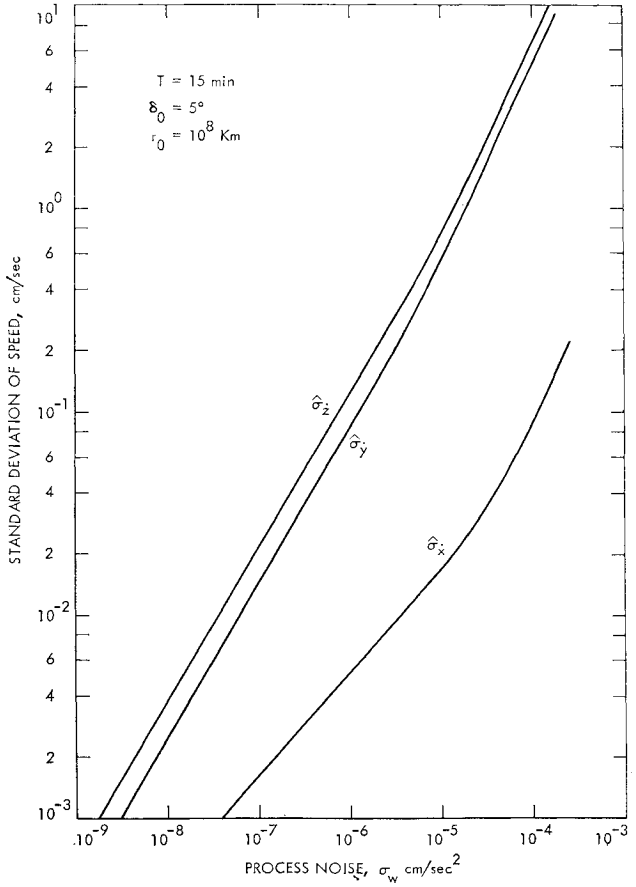

Fig. 4 Speed uncertainty vs process noise.

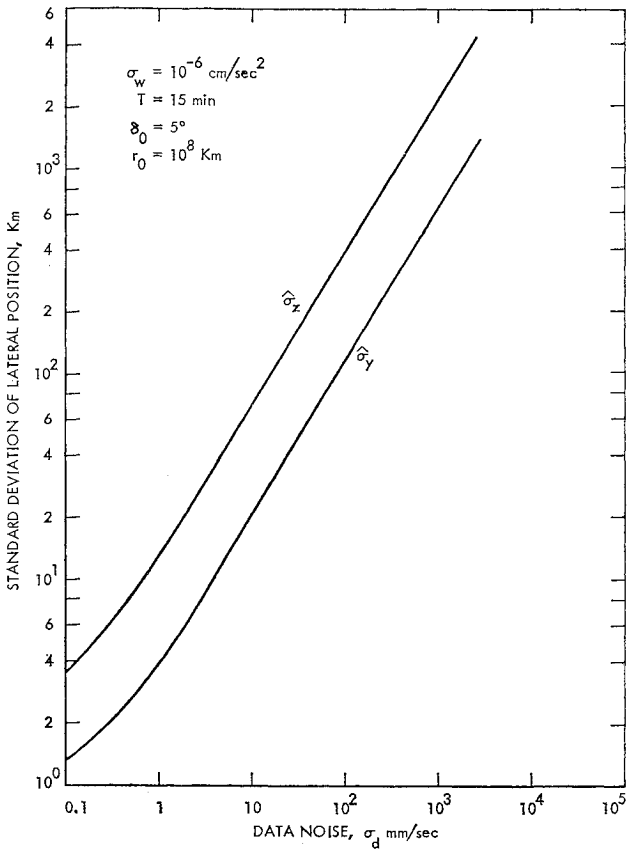

Fig. 5 Lateral position uncertainty vs data noise.

Figure 5 shows the relation between lateral position uncertainty and data noise. It shows that $\hat{\sigma}_{y,z} \sim \sigma_n^{3/4}$, as indicated in Eq. (42). Also Fig. 6 shows the relation between lateral velocity and data noise and verifies that $\hat{\sigma}_{\dot{y},\dot{z}} \sim \sigma_n^{\frac{1}{4}}$. The radial speed uncertainty $\hat{\sigma}_{\dot{x}}$ behaves quite differently from the other two parameters in Figs. 4 and 6. According to Ref. 8,

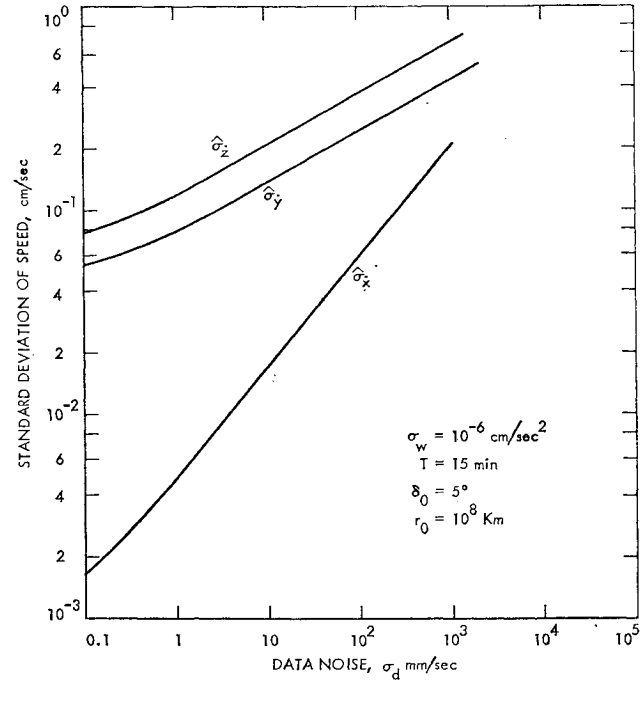

Fig. 6 Speed uncertainty vs data noise.

the steady-state solution of radial speed estimate with Doppler data is described by

$$\hat{\sigma}_{\dot{x}} \sim T(\sigma_w \sigma_d)^{\frac{1}{2}}; \quad \sigma_d = \text{standard deviation of Doppler count} \tag{44}$$

Or, in other words, the uncertainty of radial speed is proportional to the square root of the standard deviation of process noise and also of data noise. The curves of $\hat{\sigma}_{\dot{x}}$ in Figs. 4 and 6 confirm this relation.

Since σ_n in Eq. (42) represents Doppler data noise, smoothed over the sampling period T, it is related to the noise of Doppler count σ_d by

$$\sigma_n^2 = \sigma_d^2 T_c / T; \quad T_c = \text{count time} \tag{45}$$

Also, h is the partial of the Doppler data with respect to the displacement of the spacecraft. In the case of right ascension

$$h = (\omega r_s / r_0) \cos \delta_0 \tag{46}$$

Substituting these two relations into Eq. (42) yields:

$$\hat{\sigma}_\eta \approx k \sigma_w^{\frac{1}{2}} \sigma_d^{3/4} r_0^{3/4} T^{1/8} \tag{47}$$

$$k = \text{constant containing } \omega, r_s, T_c, \ldots$$

The above relation reveals the facts that

1c) Standard deviation of positional estimate is proportional to three-fourth power of radial distance r_0 to the probe and

1d) Standard deviation of positional estimate is proportional to one-eighth power of the sampling period T.

Figure 7 shows the relation of 1c in which $\hat{\sigma}_{y,z} \sim r_0^{3/4}$. Also Fig. 8 indicates the relation of $i) - d)$, namely, that $\hat{\sigma}_{y,z} \sim T^{1/8}$. Usually, this discrete period T is taken to be approximately equal to the correlation time of process noise and so, the relation $i) - d)$ implies that positional estimates are rather insensitive to the variation of correlation time of process noise in the ballistic range (lower curves). For a larger process noise they become more sensitive to T (upper curves).

II Case of $p_{11} \gg \sigma_n^2/h^2$

In this case the solution of Eq. (39) is reduced to

$$\hat{\sigma}_\eta = (p_{11})^{\frac{1}{2}} \sim \sigma_w T^2 \tag{48}$$

$$\hat{\sigma}_{\dot{\eta}} = (p_{22})^{\frac{1}{2}} \sim \sigma_w T \tag{49}$$

Therefore, 3) standard deviation of positional estimate is proportional to: a) standard deviation of process noise and b) square of discrete period T; and 4) standard deviation of speed estimate is proportional to a) standard deviation of process noise and b) discrete period T.

In Fig. 2 we observe an upward turn of curves of $\hat{\sigma}_y$ and $\hat{\sigma}_z$ in the low-thrust range and the inclination of these curves indicates that $\hat{\sigma}_{y,z} \sim \sigma_w$, as stated in 3a. Also a similar upturn of curves is seen in Fig. 3 where $\hat{\sigma}_{\dot{y},\dot{z}} \sim \hat{\sigma}_w$, confirming 4a.

Effect of Radial and Lateral Velocity

In the preceding analysis, a stationary model for the spacecraft was adopted. Namely, it was assumed that the radial distance to the probe γ, right ascension α and declination δ did not change very much from their respective original values r_0, α_0, and δ_0, over the period of estimation.

If the radial velocity $\dot{r}$ is large, the change of radial distance over the period of estimation cannot be ignored. This increase of radial distance reduces the partials with respect to lateral positions, thus effectively reducing the information content concerning these parameters. However it has been shown in the preceding section that the steady-state position

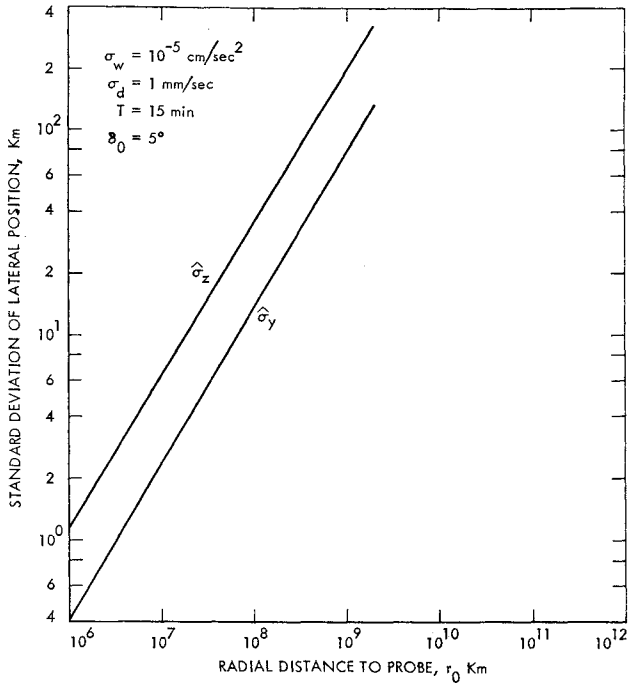

Fig. 7 Lateral position uncertainty vs distance to probe.

errors are proportional to the three-fourth power of the radial distance to the probe. If the steady-state position errors are increased by the factor of $(r/r_0)^{3/4}$, then, particularly if r is taken at the terminal time of the estimation period, the outcome will provide approximate values of steady-state solutions at the end of estimation period. This has been confirmed by comparing the results of the spectral factorization program with those of the sequential program.

When the spacecraft has significantly large lateral velocities, the problem is more complicated. The assumption of the periodically varying partials matrix does not hold any more. However, the results of the sequential program show that the aforementioned compensation with regard to radial distance improves the results of the spectral factorization program and brings it reasonably close to those of the former program, as long as the lateral velocities are not too large.

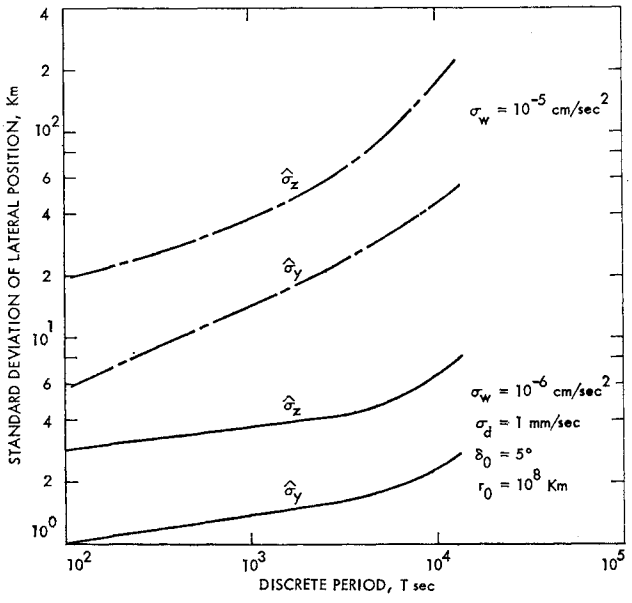

Fig. 8 Lateral position uncertainty vs discrete period.

Conclusion

The spectral factorization technique which produces the steady-state solution for Kalman filters has been extended to the periodically time-varying case for both discrete and continuous systems. Since this is an algebraic algorithm employing existing eigenvalue, eigenvector subroutines, it does not require time-consuming, expensive iterations of sequential covariance equations in order to reach the final solution. The simple and economical computer program which results is suitable for the sensitivity study which is of significant importance in formulating the navigation and guidance strategy for low-thrust missions. This sensitivity analysis will contribute greatly in establishing an optimum tracking pattern for such missions.

Appendix

Proof of Theorem 2

First assuming Eq. (12) is true, Eq. (13) is proved. When $k = 0$, Eq. (13) is valid because $B(0,0) = I$. On the other hand, according to Eqs. (10) and (8)

$$B_{11}(k+1,0) = [\Phi(k) + N\Phi_c M(k)]B_{11}(k,0) + N\Phi_c(k)B_{21}(k,0) \tag{A1}$$

$$B_{21}(k+1,0) = [\Phi(k) + N\Phi_c M(k)]B_{12}(k,0) + N\Phi_c(k)B_{22}(k,0) \tag{A2}$$

$$B_{21}(k+1,0) = \Phi_c M(k)B_{11}(k,0) + \Phi_c(k)B_{21}(k,0) \tag{A3}$$

$$B_{22}(k+1,0) = \Phi_c M(k)B_{12}(k,0) + \Phi_c(k)B_{22}(k,0) \tag{A4}$$

where

$$N = GQG',\ M = H'R^{-1}H,\ \Phi_c = (\Phi')^{-1}$$

However from Eq. (13)

$$P(L+k+1) = [B_{11}(k+1,0)T_{11}(L) + B_{12}(k+1,0)T_{21}(L)] \cdot [B_{21}(k+1,0)T_{11}(L) + B_{22}(k+1,0)T_{21}(L)]^{-1} \tag{A5}$$

When the relations of Eqs. (A1–A4) are substituted into the above equation, the following result can be derived after some matrix manipulations.

$$P(L+k+1) = \Phi(k)\{[B_{21}(k,0)T_{11}(L) + B_{22}(k,0)T_{21}(L)] \cdot [B_{11}(k,0)T_{11}(L) + B_{12}(k,0)T_{21}(L)]^{-1} + M(k)\}\Phi'(k) + N(k) \tag{A6}$$

The first term inside the larger parenthesis is nothing but $P(L+k)^{-1}$ according to Eq. (13). Thus, the above equation reduces to

$$P(L+k+1) = \Phi(k)\{P(L+k)^{-1} + M(k)\}\Phi'(k) + N(k) \tag{A7}$$

This is an alternate form of Eq. (5), if the periodicity of coefficient matrices is taken into account.

Therefore Eq. (A6) is valid at the instant $k+1$, if it is valid at k. Hence, by means of induction, Eq. (13) can be proved for all $k = 1, 2, L-1$.

Now letting $k = L$ in Eq. (13) yields

$$P(2L) = [B_{11}(L,0)T_{11}(L) + B_{12}(L,0)T_{21}(L)] \cdot [B_{21}(L,0)T_{11}(L) + B_{22}(L,0)T_{21}(L)]^{-1} \tag{A8}$$

Since T matrix is composed of eigenvectors of B, it can be described

$$B(L,0)T(L) = T(L)\Lambda \tag{A9}$$

or

$$\begin{bmatrix} B_{11}(L,0), B_{12}(L,0) \\ B_{21}(L,0), B_{22}(L,0) \end{bmatrix} \begin{bmatrix} T_{11}(L), T_{12}(L) \\ T_{21}(L), T_{22}(L) \end{bmatrix} = \begin{bmatrix} T_{11}(L), T_{12}(L) \\ T_{21}(L), T_{22}(L) \end{bmatrix} \begin{bmatrix} \Lambda_1 & 0 \\ 0 & \Lambda_2 \end{bmatrix} \quad \text{(A10)}$$

where Λ_1 is a diagonal matrix consisting of eigenvalues of B lying outside the unit circle while Λ_2 is a diagonal matrix consisting of eigenvalues lying inside the unit circle.

Then

$$B_{11}(L,0)T_{11}(L) + B_{12}(L,0)T_{21}(L) = T_{11}(L)\Lambda_1 \quad \text{(A11)}$$

$$B_{21}(L,0)T_{11}(L) + B_{22}(L,0)T_{21}(L) = T_{21}(L)\Lambda_1 \quad \text{(A12)}$$

Using these relations $P(2L)$ in Eq. (A8) can be reduced to

$$P(2L) = T_{11}(L)T_{21}(L)^{-1} = P(L) \quad \text{(A13)}$$

Therefore, after L instances, the solution of P returns to the starting value $P(L)$. This proves that $P(L)$ given by Eq. (12) is a periodic solution of the recurrence Eq. (5). The solutions at the other instants are described by Eq. (13).

References

[1] Kalman, R. E., "New Methods and Results in Linear Prediction and Estimation Theory," TR 61-1, 1961, Research Institute for Advanced Study, Baltimore, Md.

[2] Potter, J. F., "Matrix Quadratic Solutions," *Journal of SIAM Applied Mathematics*, Vol. 14, May 1966, pp. 496–501.

[3] Nishimura, T., "Spectral Factorization in Discrete Systems," *Proceedings of the 1970 IEEE Symposium on Adaptive Processes, Decision and Control*, Dec., 1970, XXIV.2.1.

[4] Vaughan, D. R., "A Nonrecursive Algebraic Solution for the Discrete Riccati Equation," *IEEE Transactions on Automatic Control*, Vol. AC-15, No. 5, Oct., 1970.

[5] Hamilton, T. W. and Melbourne, W. G., "Information Content of a Single Pass of Doppler Data from a Distant Spacecraft," *JPL Space Programs Summary No. 37–47*, Vol. II, May 1966, p. 15.

[6] Jordan, J. F., "Orbit Determination for Powered Flight Space Vehicles on Deep Space Missions," *Journal of Spacecraft and Rockets*, Vol. 6, No. 5, May 1969, pp. 545–551.

[7] Jordan, J. F. and Rourke, K. H., "Guidance and Navigation for Solar Electric Interplanetary Missions," *Journal of Spacecraft and Rockets*, Vol. 8, No. 9, Sept. 1971, pp. 920–927.

[8] Nishimura, T., "Error Bounds of Continuous Kalman Filters and the Application to Orbit Determination Problems," *IEEE Transactions on Automatic Control*, Vol. AC 12, No. 3, June 1967, pp. 268–275.